UCSB Graphene-Nanoribbon (GNR) Interconnect Compact Model (VERSION = 2.0.0)

Junkai Jiang, Jiahao Kang, Wei Cao and Prof. Kaustav Banerjee

Table of Contents

1. Introduction 2

2. Terminal and Distributed Circuit definition 3

3. User-defined parameters 4

4. GNR Interconnect Model 5

a. Quantum Contact Resistance 5

b. GNR Resistance 5

c. GNR Capacitance 7

d. GNR Inductance 8

5. DC Circuit Simulation 9

6. Transient Circuit Simulation..... 11

7. Calibration with Electrical Measurements..... 12

8. To-dos and Summary 12

9. References..... 13

1. Introduction

As the (local) interconnect dimension scales down to sub-20 nm, the rapidly increasing metal resistance by barrier layer and surface and grain boundary scatterings, and the diminishing current carrying capacity by self-heating and Joule-heating, the metal (Cu) interconnect cannot meet the requirements from the circuit performance. Graphene nanoribbon interconnect is an excellent candidate for the interconnect, mainly because of its high current carrying capacity [1][2][3][4]. Intercalation doped graphene nanoribbon (GNR) interconnect was first proposed by [1][2], and was recently demonstrated to offer excellent circuit performance and energy efficiency improvements [3], and was demonstrated with more than 100× reliability improvement w.r.t. Cu interconnects [4]. UCSB GNR interconnect compact model describes the circuit-level behavior of the (intercalation) doped GNR interconnect. This model is based on a distributed RLC circuit, in which carrier mean free path (l_D), GNR doping doping (Fermi) level (E_F), number of layers (*N_L*), edge specularity (*p*) and low-k dielectric constant (*eps*) are considered. The model was originally published by our group in [2]. By using a simple tight-binding model and the linear response Landauer formula, the resistance of GNR is derived. Quantum contact resistance is the minimum contact resistance to the 2-dimensional system (GNR), and is considered in the model. In addition to the resistance, the capacitance (electrostatic capacitance and quantum capacitance) and inductance (magnetic inductance and kinetic inductance) are considered to satisfy the transient simulation requirements. By implementing the model in Verilog-A, our GNR interconnect model is compatible with both DC and transient SPICE simulations.

2. Terminal and Distributed Circuit Definition

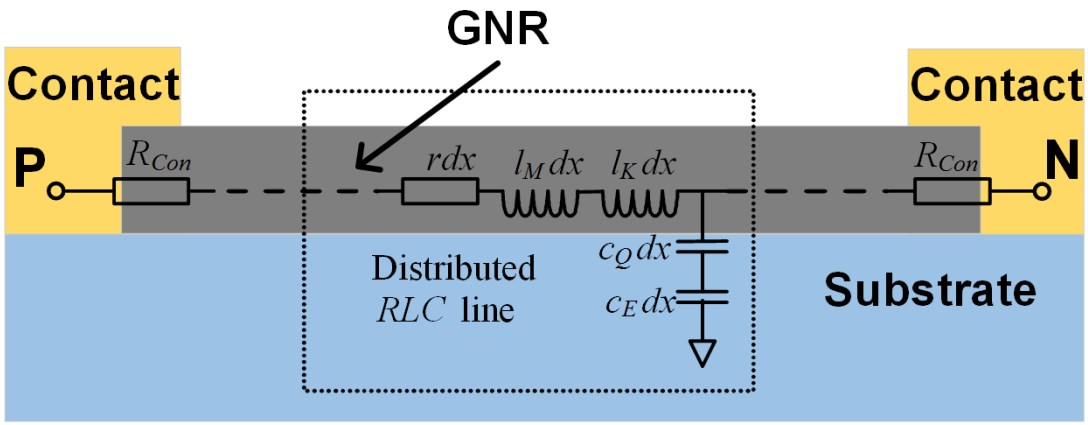

Figure 1 Schematic of a GNR interconnect and corresponding RLC distributed circuit model

This model provides two external terminals, ***P*** and ***N***, that represent the positive and negative terminals of a GNR interconnect. A distributed *RLC* equivalent circuit for GNRs is considered. $\boldsymbol{R_{Con}}$ is the GNR contact resistance, ***r*** is the GNR resistance per unit length, $\boldsymbol{l_M}$ and $\boldsymbol{l_K}$ are the GNR magnetic inductance and kinetic inductance per unit length, respectively, and $\boldsymbol{c_Q}$ and $\boldsymbol{c_E}$ are the GNR quantum capacitance and electrostatic capacitance per unit length, respectively. Notice that terminal **P** and **N** are symmetric, i.e., completely interchangeable.

3. User-defined Parameters

Parameter	Default Value	Definition
l	1e-6 m	Length of GNR
w	1e-7 m	Width of GNR
N_L	1	Number of layers of GNR
dope	0 m^{-3}	Dopant concentration in GNR
E_F	0 eV	GNR Fermi-level
l_D	1e-6 m	Carrier mean free path (MFP)
edge_p	1	GNR edge specularity
eps	2.0	Surrounding dielectric constant
Rcon	0 (If default value is used, quantum contact resistance is calculated and used in the model)	User defined contact resistance

4. GNR Interconnect Model

The GNR interconnect model considers contact resistance, GNR resistance, inductance and capacitance. The contact resistance can either be determined by the user (by setting a non-zero value in *Rcon*), or can be default value that is the minimum theoretical contact resistance. The GNR resistance (r), quantum capacitance (c_Q) and kinetic inductance (l_K) are modeled as adopted from [2]. The electrostatic capacitance (c_E) and magnetic inductance (l_M) are calculated from analytical solutions reported in [5] and [6], respectively. For more accurate modeling, they can also be calculated by field solvers and inserted in the GNR model.

a. Quantum Contact Resistance

The quantum contact resistance is the lower limit of contact resistance in GNR interconnects, and is defined as [2]

$$R_Q = (h/2q^2)/N_{ch}N_{layer} \tag{1}$$

where N_{ch} is the number of conducting channels (modes) in one GNR layer, N_{layer} is the number of GNR layers, h is the Planck's constant and q is electron charge. The number of conducting channels (modes) N_{ch} can be calculated as

$$N_{ch} = N_{ch,electron} + N_{ch,hole} = \sum_n \left[1+\exp\left(\frac{E_{n,electron}-E_F}{k_BT}\right)\right]^{-1} + \sum_n \left[1+\exp(\frac{E_F-E_{n,hole}}{k_BT})\right]^{-1} \tag{2}$$

where $E_{n,electron}$ ($E_{n,hole}$) is the minimum (maximum) energy of the nth conduction (valence) subband.

b. GNR Resistance

Based on the linear response (small voltage drop along the length) Laudauer formula, the conductance of the nth conduction mode in a single GNR layer G_n can be expressed as

$$G_n = 2q^2/h \cdot \int T_n(E)(-\partial f_0/\partial E)dE \tag{3}$$

$$f_0(E) = \{1 + \exp[(E - E_F)/k_B T]\}^{-1} \tag{4}$$

where $T_n(E)$ is the transmission coefficient of carriers, $f_0(E)$ is the Fermi-Dirac distribution function, E_F is the Fermi level, k_B is Boltzmann's constant, and T is the temperature. Considering the edge scattering coefficient p. And p = 1 is for fully specular, and p = 0 is for fully diffusive. The transmission coefficient $T_n(E)$ can be determined by

$$\frac{1}{T_n(\mathrm{E})} = 1 + \frac{L}{l_D \cos\theta} + \frac{L(1-p)}{w\cot\theta} \approx \frac{L}{l_D \cos\theta} + \frac{L(1-p)}{w\cot\theta} \tag{5}$$

Where L is the GNR length, l_D is the carrier mean free path that does not considers edge scattering events, w is the GNR width, and cotθ is the ratio of longitudinal (along the wire length) to transverse (across the wire width) velocities. In (4), the term "1" is due to quantum conductance, which can be ignored when $L >> l_D$.

The total conductance of a single GNR layer is the summation of conductance of electrons and holes, as in (5).

$$G_{total} = \sum_n G_n(\text{electrons}) + \sum_n G_n(\text{holes}) \tag{6}$$

And the summation in (5) can be transformed to an integration form as follows:

$$G_{total} = \frac{2}{\Delta E_n}\left[\int_0^{\infty} G_n(\text{electrons})\,\mathrm{d}\,E_n + \int_{-\infty}^{0} G_n(\text{holes})\,\mathrm{d}\,E_n\right] \tag{7}$$

The electrical conduction contributed by electron can be derived as

$$\int_0^{\infty} G_n(\text{electrons})\,\mathrm{d}\,E_n = \frac{2q^2}{h}\int_0^{\infty} E\left(-\frac{\partial f_0}{\partial E}\right)dE \int_0^{E} \frac{1}{E} T_n(E)\,dE_n \tag{8}$$

where

$$\int_0^{E} \frac{1}{E} T_n(E)\,dE_n = \int_0^{\pi/2} \frac{1}{L}\left(\frac{1}{l_D \cos\theta} + \frac{1-p}{w\cot\theta}\right)^{-1} \cos\theta\, d\theta = \frac{1}{L}\int_0^{\pi/2}\left(\frac{1}{l_D} + \frac{\sin\theta(1-p)}{w}\right)^{-1} \cos^2\theta\, d\theta \tag{9}$$

$$\int_0^{\infty} E\left(-\frac{\partial f_0}{\partial E}\right)dE = k_B T \ln(1 + \exp(\frac{E_F}{k_B T})) \tag{10}$$

The electron contributed conduction can be further derived as

$$\int_0^{\infty} G_n(\text{electrons})\,\mathrm{d}E_n = \frac{2q^2}{h} k_B T \ln\left(1+\exp\left(\frac{E_F}{k_B T}\right)\right)\frac{1}{L}\int_0^{\pi/2}\left(\frac{1}{l_D}+\frac{\sin\theta(1-p)}{w}\right)^{-1}\cos^2\theta d\theta \quad (11)$$

Similarly, the hole contributed conduction can be derived as

$$\int_0^{\infty} G_n(holes)\,\mathrm{d}E_n = \frac{2q^2}{h} k_B T \ln\left(1+\exp\left(\frac{-E_F}{k_B T}\right)\right)\frac{1}{L}\int_0^{\pi/2}\left(\frac{1}{l_D}+\frac{\sin\theta(1-p)}{w}\right)^{-1}\cos^2\theta d\theta \quad (12)$$

Therefore, the total GNR electrical conductance is

$$G_{total} = \frac{1}{L}\frac{4w}{hv_f}\frac{2q^2}{h} k_B T 2\ln\left(2\cosh\left(\frac{E_F}{2k_B T}\right)\right)\int_0^{\pi/2}\left(\frac{1}{l_D}+\frac{\sin\theta(1-p)}{w}\right)^{-1}\cos^2\theta d\theta \quad (13)$$

c. GNR Capacitance

The GNR capacitance consists of electrostatic capacitance ($c_{electrostatic}$) and quantum capacitance (c_Q). By assuming the wire pitch = 2 × wire width (w_{GNR}), or wire spacing (S) = wire width (w_{GNR}), intermetal dielectric thickness (H_{diel}) = 2 × wire thickness (t_{GNR}), the GNR interconnect electrostatic capacitance is estimated as

$$c_{electrostatic} = c_{ground} + c_{intra} + c_{inter} \quad (14)$$

where c_{ground}, c_{intra} and c_{inter} are wire to ground capacitance, intralayer capacitance and interlayer capacitance, respectively [5].

$$c_{ground} = \varepsilon_r\varepsilon_0\left(\frac{w_{GNR}}{H_{diel}} + 3.28\left(\frac{t_{GNR}}{t_{GNR}+2H_{diel}}\right)^{0.023} + \left(\frac{S}{S+2H_{diel}}\right)^{1.16}\right) \quad (15)$$

$$c_{intra} = \varepsilon_r\varepsilon_0\left(\begin{array}{l} 1.064\left(\frac{t_{GNR}}{S}\right)\left(\frac{t_{GNR}+2H_{diel}}{t_{GNR}+2H_{diel}+0.5S}\right)^{0.695} + \\ \left(\frac{w_{GNR}}{w_{GNR}+0.8S}\right)^{1.4148}\left(\frac{t_{GNR}+2H_{diel}}{t_{GNR}+2H_{diel}+0.5S}\right)^{0.804} + \\ 0.831\left(\frac{w_{GNR}}{w_{GNR}+0.8S}\right)^{0.055}\left(\frac{2H_{diel}}{2H_{diel}+0.5S}\right)^{3.542} \end{array}\right) \quad (16)$$

$$c_{inter} = \varepsilon_r \varepsilon_0 \left(\frac{w_{GNR}^2}{H_{diel}} + \left(\begin{array}{l} 1 - 0.326 \exp\left(\frac{-t_{GNR}}{0.133S} \right) - 0.959 \exp\left(\frac{-S}{1.966 H_{diel}} \right) \\ \left(3.7652 w_{GNR} \left(\frac{S}{S + 0.01 H_{diel}} \right)^{0.2} + 2.28 S \left(\frac{w_{GNR}}{H_{diel}} \right)^{0.182} \right) \end{array} \right) \right) \quad (17)$$

The quantum capacitance (c_Q) is calculated by

$$c_Q = N_{layer} N_{ch} 4q^2 / h v_f \quad (18)$$

where v_f is the Fermi velocity, which is estimated as 10^6 m/s in the model. The total GNR capacitance is

$$c_{total} = \frac{c_{electrostatic} c_Q}{c_{electrostatic} + c_Q} \quad (19)$$

d. GNR Inductance

The GNR inductance consists of magnetic inductance (l_M) and kinetic inductance (l_K). To estimate the magnetic inductance, the model assumes that the spacing between signal and the nearest ground wire (SS) = 2 × wire pitch. The magnetic inductance can be calculated by analytical expression [6]

$$l_M = 3 \ln \left(\frac{SS + w_{GNR}}{w_{GNR} + t_{GNR}} \pi \right) - \ln 2 + 0.75 \quad (20)$$

The inductance is calculated as [2]

$$l_K = (h / 4q^2 v_f) / N_{layer} N_{ch} \quad (21)$$

And the total GNR inductance is

$$l_{total} = l_M + l_K \quad (22)$$

5. DC Circuit Simulation

For DC simulation (GNR_DC.sp), the right circuit (Fig. 2) is applied. The DC simulation measures the resistance of GNR interconnect. The GNR is set to be 100 nm long, 20 nm wide, 10 layers (~ 5 nm thick), of a doping level of $|E_F|$ = 0.6 eV, edge specularity p = 0.8. Fig. 3, Fig. 4, Fig. 5 and Fig. 6 plot the measured GNR interconnect resistance from Hspice simulations for different GNR width (w_{GNR}), edge specularity (p), carrier diffusion length (l_D, without considering edge scatterings) and doping level ($|E_F|$), respectively.

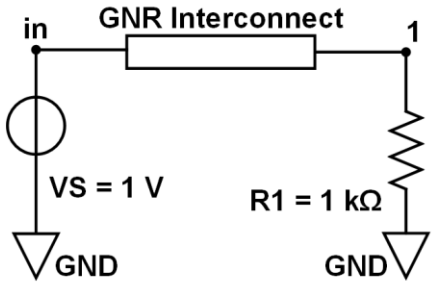

Figure 2 Circuit for DC simulations

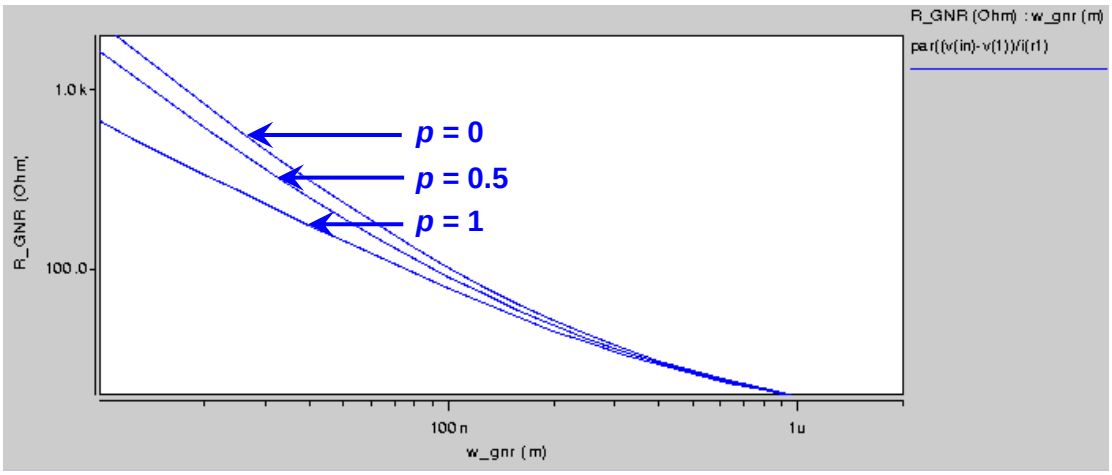

Figure 3 R_{GNR} vs. GNR width w_{GNR} for edge specularity of p = 0, 0.5 and 1.

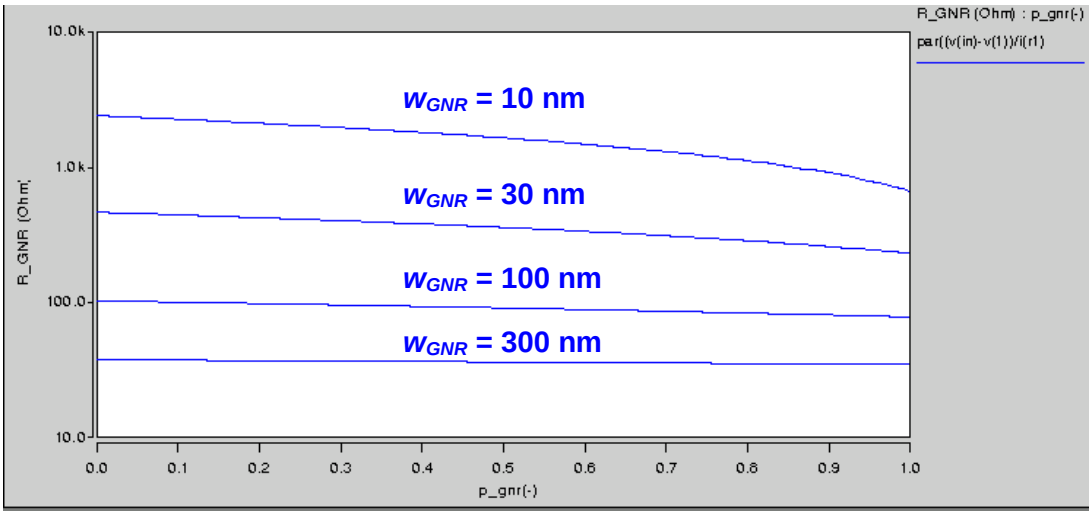

Figure 4 R_{GNR} vs. edge specularity (p) for GNR width w_{GNR} = 10 nm, 30 nm, 100 nm and 300 nm.

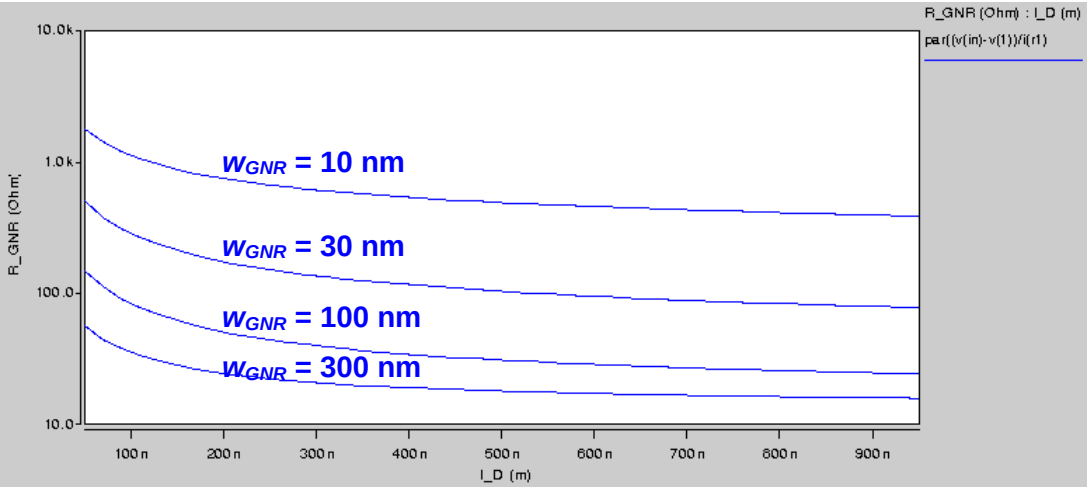

Figure 5 R_{GNR} vs. carrier diffusion length (l_D) for GNR width w_{GNR} = 10 nm, 30 nm, 100 nm and 300 nm.

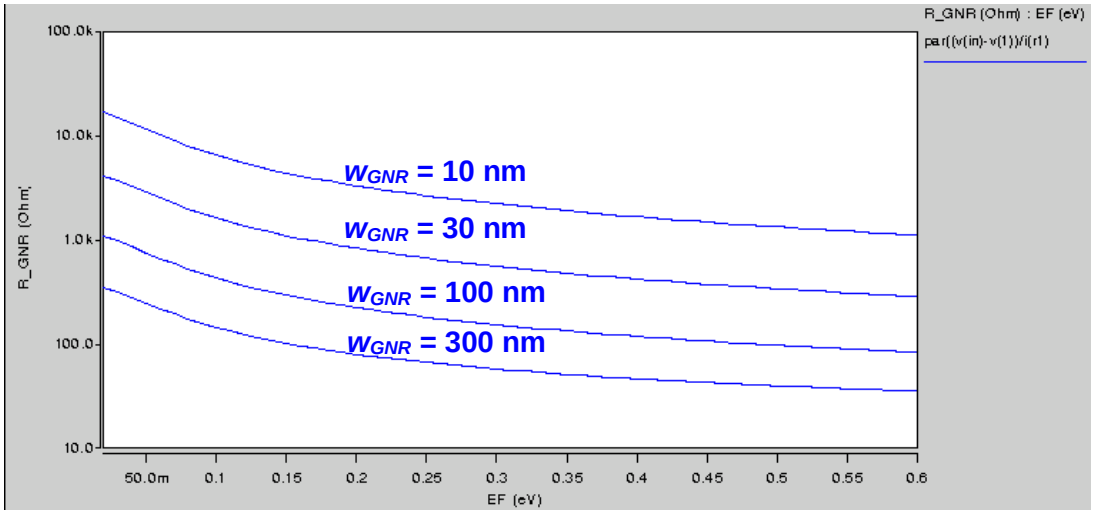

Figure 6 R_{GNR} vs. doping level diffusion length ($|E_F|$) for GNR width w_{GNR} = 10 nm, 30 nm, 100 nm and 300 nm.

6. Transient Circuit Simulation

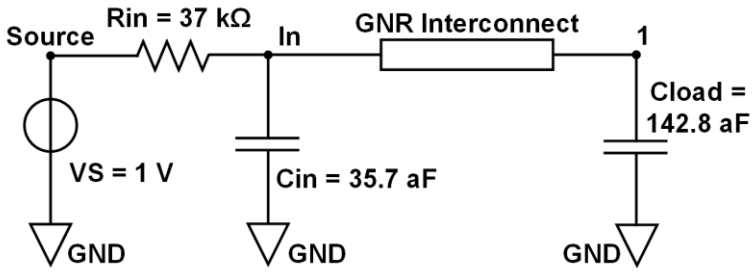

Figure 7 Circuit for DC simulations

Fig. 7 shows the schematic of the circuit for transient simulation. In the transient simulation (GNR_TR.sp), the GNR is set to be 100 nm long, 20 nm wide, 10 layers (~ 5 nm thick), of a doping level of $|E_F|$ = 0.6 eV, edge specularity p = 0.8. The dielectric constant of the surrounding dielectric is 2.0. Fig. 8 plot the measured output voltage and source voltage from the Hspice transient simulations, and the 10%-90% rise time is 15 ps.

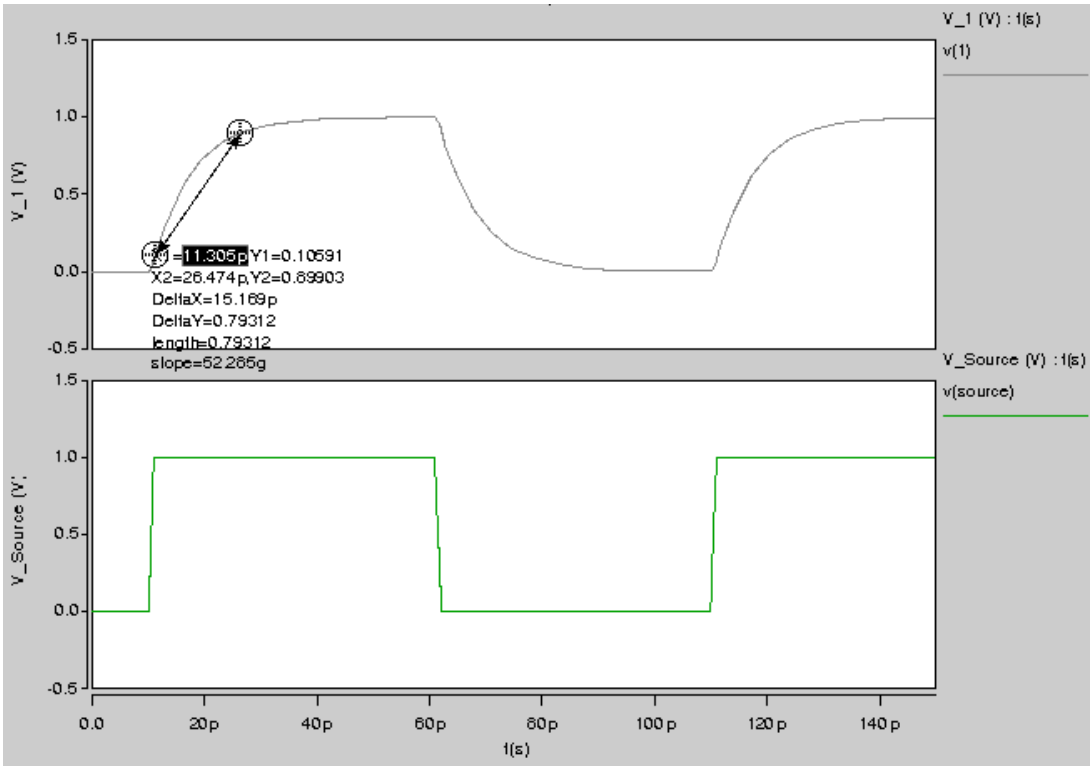

Figure 8 Source voltage *(V(Source)) and* output voltage *(V(1))*. The 10%-90% rise time of the output voltage is measured as 15 ps.

7. Calibration with Electrical Measurements

As reported in [3], we fabricated undoped ($|E_F| = 0$) and doped ($|E_F| > 0$) GNR interconnect 4-probe test structures (Fig. 9(a)(b)). Fig. 9(c) shows the fitted GNR model with measured data on the undoped GNR. Fig. 9(d)(e) shows the measured resistivity of 10-hour doped GNR and the extracted doping level ($|E_F|$), respectively.

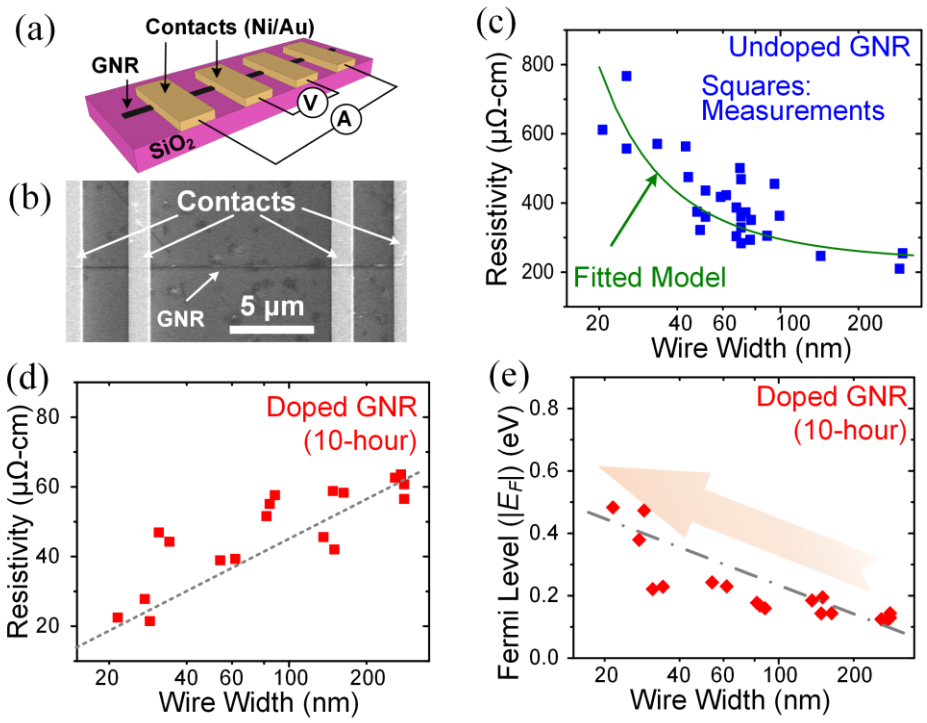

Figure 9 (a) Schematic of 4-probe test structure. (b) Scanning electron microscope (SEM) image of test structure. (c) Fitted model with electrical measurement data for undoped GNR. (d) Measured resistivity for 10-hour doped GNR. (e) Extracted doping level for 10-hour doped GNR.

8. To-dos and Summary

This GNR compact model considers the multiple scattering effects in GNR, including edge scatterings and non-edge scatterings (e.g. phonon-electron scatterings). It also considers (intercalation) doping level that effectively increases the carrier concentration in GNR, width-dependency of GNR resistance from the edge scatterings, and GNR parasitic capacitance and inductance, as well as the contact resistance. For a more accurate modeling of sub-10 nm width GNR interconnect, bandgap (E_g) opening as modeled in [2][3], needs to be considered. However, for a relatively high doping level ($|E_F| >> E_g / 2$), the bandgap opening is not a dominant factor in determining the GNR resistance. The temperature coefficient of resistance (TCR) and self-heating of GNR interconnect was reported in [4], and can be included in this compact model in the future.

9. References

[1] C. Xu, H. Li and K. Banerjee, "Graphene Nano-Ribbon (GNR) Interconnects: A Genuine Contender or a Delusive Dream?" *IEEE International Electron Devices Meeting (IEDM)*, San Francisco, Dec. 15-17, 2008.

[2] C. Xu, H. Li and K. Banerjee, "Modeling, Analysis, and Design of Graphene Nano-Ribbon Interconnects," *IEEE Trans. on Electron Devices*, vol. 56, no. 8, pp. 1567-1578, 2009.

[3] J. Jiang, J. Kang, W. Cao, X. Xie, H. Zhang, J. H. Chu, W. Liu and K. Banerjee, "Intercalation Doped Multilayer-Graphene-Nanoribbons for Next-Generation Interconnects," *Nano Letters*, vol. 17, no. 3, pp. 1482-1488, 2016.

[4] J. Jiang, J. Kang and K. Banerjee, "Characterization of Self-Heating and Current-Carrying Capacity of Intercalation Doped Graphene-Nanoribbon Interconnects," *IEEE International Reliability Physics Symposium (IRPS)*, Monterey, April 4-6, 2017.

[5] J. H. Chern, J. Huang, L. Arledge, P. C. Li and P. Yang, "Multilevel Metal Capacitance Models for CAD Design Synthesis Systems," *IEEE Electron Device Letters*, vol. 13, no. 1, pp. 32-34, 1992.

[6] X. Qi, B. Kleveland, Z. Yu, S. Wong, R. Dutton and T. Young, "On-Chip Inductance Modeling of VLSI Interconnects," *IEEE International Solid-State Circuits Conferenc*e, Feb. 9, 2000.